Journal of Molecular Structure 1012 (2012) 131–136

Contents lists available at SciVerse ScienceDirect

Journal of Molecular Structure

journal homepage: www.elsevier.com/locate/molstruc

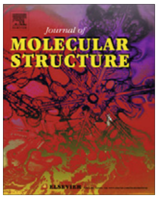

Dicarboxylate-controlled three Zn(II) coordination polymers incorporating flexible 1,2-bis(imidazol-1′-yl)ethane ligand: Syntheses, structures, thermal stabilities and photoluminescent properties

Hong-Jun Hao [a,1], Di Sun [b,*,1], Fu-Jing Liu [a], Rong-Bin Huang [a,*], Lan-Sun Zheng [a]

[a] State Key Laboratory for Physical Chemistry of Solid Surfaces, Department of Chemistry, College of Chemistry and Chemical Engineering, Xiamen University, Xiamen, Fujian 361005, China
[b] School of Chemistry and Chemical Engineering, Shandong University, Jinan, Shandong 250100, China

ARTICLE INFO

Article history:
Received 12 November 2011
Received in revised form 18 December 2011
Accepted 19 December 2011
Available online 5 January 2012

Keywords:
Zinc(II)
1,2-Bis(imidazol-1′-yl)ethane
Dicarboxylate
Photoluminescence

ABSTRACT

Three mixed-ligand Zn(II) coordination polymers (CPs) of the formula $\{[Zn_2(bime)_2(adip)_2]\cdot(H_2O)_5\}_n$ (**1**), $\{[Zn(bime)(ipa)]\cdot(H_2O)_3\}_n$ (**2**), $\{[Zn(bime)(tpa)]\cdot(H_2O)\cdot(CH_3OH)\}_n$ (**3**) (bime = 1,2-bis(imidazol-1′-yl)ethane, H_2adip = adipic acid, H_2ipa = isophthalic acid and H_2tpa = terephthalic acid) were synthesized. All CPs have been characterized by element analysis, powder X-ray diffraction (PXRD), IR and X-ray single-crystal diffraction. Complexes **1** and **2** exhibit similar wavy two-dimensional (2D) sheets with 4^4-**sql** topology. Compared to **1**, complex **2** contains a larger window owing to the different conformation of bime ligand. In both **1** and **2**, we observed 1D water chain filling in the 4^4-**sql** net. In **3**, the bime acts as a bidentate ligand and the tpa adopts a μ_2-η^1,η^1 coordinated mode which links the Zn(II) ions to form a 2D 6^3-**hcb** net. The results suggest that the dicarboxylates play crucial roles in the formation of the different structures. In addition, the thermal stabilities and the photoluminescence properties of them were also investigated.

1. Introduction

Particular attention has been recently devoted to coordination polymers (CPs) due to not only their undisputed structural beauty but also promising applications in the fields of catalysis, storage, conduction, luminescence, conductivity, non-linear optics (NLOs), ferroelectricity and magnetism [1–13]. The construction of CPs depends on the combination of several factors, such as solvent system [14–16], counteranion [17–20], pH value of the solution [21–23], reaction temperature, ratio of ligand to metal ion, coordination geometry of central metals and organic ligands [24]. Thus, understanding how these considerations affect metal coordination and influence supramolecular assembly is at the forefront of controlling coordination supramolecular arrays.

To the best of our knowledge, the bime, bearing alkyl spacers is a good choice of N-donor ligands, the flexible nature of spacers allows the ligands to bend and rotate when it coordinates to metal centers, and this often causes the structural diversity. As a consequence of the free rotation of the ethyl group, it possesses *gauche* and *anti* conformations which favor the possibility of generating fascinating structures. However, as indicated by CSD (Cambridge Structure Database) survey with the help of ConQuest version 1.3 [25,26], there are only four Zn/bime CPs. In view of above consideration, herein we wish to report the syntheses, crystal structures, characterizations and photoluminescences of three Zn(II) mixed-ligand CPs, namely, $\{[Zn_2(bime)_2(adip)_2]\cdot(H_2O)_5\}_n$ (**1**), $\{[Zn(bime)(ipa)]\cdot(H_2O)_3\}_n$ (**2**), $\{[Zn(bime)(tpa)]\cdot(H_2O)\cdot(CH_3OH)\}_n$ (**3**) (bime = 1,2-bis(imidazol-1′-yl)ethane, H_2adip = adipic acid, H_2ipa = isophthalic acid and H_2tpa = terephthalic acid).

2. Experimental

2.1. Materials and physical measurements

All the reagents and solvents employed were commercially available and used as received without further purification. Infrared spectra were recorded on a Nicolet AVATAT FT-IR330 spectrometer as KBr pellets in the frequency range 4000–400 cm^{-1}. The elemental analyses (C, H, N contents) were determined on a CE instruments EA 1110 analyzer. Photoluminescence measurements were performed on a Hitachi F-7000 fluorescence spectrophotometer with solid powder on a 1 cm quartz round plate. Thermogravimetric analyses were performed on a NETZSCH TG 209 F1 Iris® Thermogravimetric Analyser from 30 to 800 °C at a heating rate 10 °C/min under the N_2 atmosphere (20 mL/min). X-ray powder diffractions were measured on a Panalytical X-Pert pro diffractometer with Cu Kα radiation.

---

* Corresponding authors. Fax: +86 592 2183047.
E-mail addresses: dsun@sdu.edu.cn (D. Sun), rbhuang@xmu.edu.cn (R.-B. Huang).
[1] These authors contributed equally to this work.

0022-2860/$ - see front matter © 2012 Elsevier B.V. All rights reserved.
doi:10.1016/j.molstruc.2011.12.030

2.2. Synthesis of complex $\{[Zn_2(bime)_2(adip)_2]\cdot(H_2O)_5\}_n$ (**1**)

A mixture of $Zn(OOCCH_3)_2\cdot 2H_2O$ (43.8 mg, 0.2 mmol), bime (32.4 mg, 0.2 mmol) and H_2adip (26.4 mg, 0.2 mmol) was treated in DMF-H_2O mixed solvent (6 mL, *v*/*v*: 2/1) under ultrasonic irradiation at ambient temperature. Then aqueous NH_3 solution (25%, 10 d) was dropped into the mixture to give a clear solution under ultrasonic treatment. The resultant solution was allowed to evaporate slowly in darkness at room temperature for several days to give pale-yellow crystals of **1** (yield: 56%, based on $Zn(OOCCH_3)_2\cdot 2H_2O$). Anal. Calc. (found) for $Zn_2C_{28}H_{45}N_8O_{13}$: C, 40.40 (40.34); H, 5.45 (5.54); N, 13.46 (13.35)%. IR (KBr): $\nu(cm^{-1})$ = 3453 (s), 3123 (s), 2940 (w), 1571 (s), 1535 (w), 1425 (m), 1241 (w), 1107 (w), 960 (w), 643 (w).

2.3. Synthesis of complex $\{[Zn(bime)(ipa)]\cdot(H_2O)_3\}_n$ (**2**)

The synthesis of **2** was similar to that of **1**, but with H_2ipa (42.4 mg, 0.2 mmol) in place of H_2adip in DMF-H_2O mixed solvent (6 mL, *v*/*v*: 2/1) under ultrasonic irradiation at ambient temperature. Pale-yellow crystals of **2** were obtained in 75% yield based on $Zn(OOCCH_3)_2\cdot 2H_2O$. Anal. Calc. (found) for $ZnC_{16}H_{20}N_4O_7$: C, 43.11 (43.04); H, 4.52 (4.44); N, 12.57 (12.45)%. IR (KBr): $\nu(cm^{-1})$ = 3429 (s), 3319 (s), 3123 (s), 1608 (s), 1559 (s), 1376 (s), 1241 (w), 1107 (w), 948 (w), 740 (m), 643 (w).

2.4. Synthesis of complex $\{[Zn(bime)(tpa)]\cdot(H_2O)\cdot(CH_3OH)\}_n$ (**3**)

The synthesis of **3** was similar to that of **1**, but with H_2tpa (42.4 mg, 0.2 mmol) in place of H_2adip in DMF-H_2O mixed solvent (6 mL, *v*/*v*: 2/1) under ultrasonic irradiation at ambient temperature. Pale-yellow crystals of **3** were obtained in 62% yield based on $Zn(OOCCH_3)_2\cdot 2H_2O$. Anal. Calc. (found) for $ZnC_{17}H_{20}N_4O_6$: C, 46.22 (46.14); H, 4.56 (4.47); N, 12.68 (12.65)%. IR (KBr): $\nu(cm^{-1})$ = 3429 (s), 3123 (s), 1596 (s), 1376 (s), 1229 (w), 1107 (w), 960 (w), 826 (w), 735 (w), 643 (w).

3. X-ray crystallography

Single crystals of the complexes **1–3** with appropriate dimensions were mounted on a glass fiber and used for data collection. Data were collected on a Bruker-AXS CCD diffractometer equipped with a graphite-monochromated Mo Kα radiation source (λ = 0.71073 Å) for **1** and **3**, and a Rigaku R-AXIS RAPID Imaging Plate single-crystal diffractometer equipped with a graphite-monochromated Mo Kα radiation source (λ = 0.71073 Å) for **2**. The crystal structures were solved by direct methods and refined with the full-matrix least-squares technique on F^2 using the SHELXS-97 and SHEXL-97 programs [27,28]. The crystallographic details of **1–3** are summarized in Table 1. Selected bond lengths and angles for **1–3** are collected in Table 2.

4. Results and discussion

4.1. Syntheses and IR

The syntheses of complexes **1–3** were carried out in the room temperature. The infrared spectra and elemental analyses of **1–3** are fully consistent with their formations. The IR spectra (Fig. S4) of complexes **1–3** show features attributable to the carboxylic group stretching vibrations. No band in the region 1690–1730 cm^{-1}, indicates complete deprotonation of the carboxyl groups. The characteristic bands of the carboxylic groups are shown in the range 1541–1625 cm^{-1} for asymmetric stretching and 1345–1492 cm^{-1} for symmetric stretching. The splitting of ν_{as}(COO) indicates the different coordination modes of carboxyl group [29], being in agreement with their crystal structures.

Table 1
Crystallographic data for complexes **1**–3.

Complexes	**1**	**2**	**3**
Formula	$Zn_2C_{28}H_{45}N_8O_{13}$	$ZnC_{16}H_{14}N_4O_7$	$ZnC_{17}H_{20}N_4O_6$
M_r	832.46	439.70	441.74
Crystal system	Monoclinic	Monoclinic	Triclinic
Space group	*Pc*	*P*2(1)/c	*P*-1
a (Å)	8.2138(16)	10.231(2)	9.4794(17)
b (Å)	17.491(3)	21.874(4)	10.3579(19)
c (Å)	12.260(2)	8.8151(18)	10.682(2)
α (deg)	90.00	90.00	74.805(3)
β (deg)	90.234(4)	103.52(3)	73.450(3)
γ (deg)	90.00	90.00	76.959(3)
Z	2	4	2
V (Å^3)	1761.3(6)	1918.1(6)	957.2(3)
D_c (g cm^{-3})	1.570	1.523	1.533
μ (mm^{-1})	1.436	1.326	1.325
F (000)	866	896	456
No. of unique reflns	5121	3728	3281
No. of obsd reflns [$I > 2\sigma(I)$]	5019	2252	3194
Parameters	461	254	262
GOF	0.816	1.088	1.099
Final *R* indices [$I > 2\sigma(I)$]^{a,b}	R_1 = 0.0350,	R_1 = 0.0758	R_1 = 0.0284
	wR_2 = 0.1052	wR_2 = 0.1612	wR_2 = 0.0788
R indices (all data)	R_1 = 0.0357 wR_2 = 0.1060	R_1 = 0.1413 wR_2 = 0.2379	R_1 = 0.0290, wR_2 = 0.0792
Largest difference peak and hole (e Å^{-3})	0.563 and −0.320	1.396 and −1.602	0.701 and −0.790

[a] $R_1 = \sum \|F_o| - |F_c\| / \sum |F_o|$.

[b] $wR_2 = \left[\sum w(F_o^2 - F_c^2)^2 \Big/ \sum w(F_o^2)^2\right]^{0.5}$.

Table 2
Selected bond distances (Å) and angles (°) for **1–3**.

*Complex **1***			
Zn1–O3^{i}	1.965(3)	Zn2–O7	1.968(3)
Zn1–O5	1.983(3)	Zn2–N8	1.983(4)
Zn1–N1	1.983(4)	Zn2–O2	2.019(3)
Zn1–N3^{ii}	2.024(4)	Zn2–N6^{iii}	2.041(4)
O3^{i}–Zn1–O5	105.43(14)	O7–Zn2–N8	126.58(16)
O3^{i}–Zn1–N1	125.33(17)	O7–Zn2–O2	102.09(14)
O5–Zn1–N1	111.09(15)	N8–Zn2–O2	116.89(14)
O3^{i}–Zn1–N3^{ii}	100.19(16)	O7–Zn2–N6^{iii}	96.58(14)
O5–Zn1–N3^{ii}	99.04(16)	N8–Zn2–N6^{iii}	109.30(18)
N1–Zn1–N3^{ii}	112.26(18)	O2–Zn2–N6^{iii}	100.93(16)
Symmetry codes: (i) *x*, *y* + 1, *z*; (ii) *x* + 1, *y*, *z*; (iii) *x* − 1, *y*, *z*			
*Complex **2***			
Zn1–N3	1.992(7)	Zn1–O3^{ii}	2.021(6)
Zn1–N2^{i}	1.994(7)	Zn1–O2	1.995(6)
N3–Zn1–N2^{i}	123.4(3)	O2–Zn1–O3^{ii}	100.7(2)
N3–Zn1–O2	103.1(2)	N3–Zn1–O3^{ii}	110.6(2)
N2^{i}–Zn1–O2	105.3(3)	N2^{i}–Zn1–O3^{ii}	110.7(3)
Symmetry codes: (i) −*x* + 1, *y* + 1/2, −*z* + 1/2; (ii) *x* − 1, *y*, *z*			
*Complex **3***			
Zn1–O3	1.9494(15)	Zn1–N4^{i}	1.9957(19)
Zn1–O2	1.9901(15)	Zn1–N1	2.0101(19)
O3–Zn1–O2	107.20(7)	O3–Zn1–N1	97.21(7)
O3–Zn1–N4^{i}	113.71(7)	O2–Zn1–N1	110.87(7)
O2–Zn1–N4^{i}	115.31(7)	N4^{i}–Zn1–N1	111.05(8)
Symmetry codes: (i) −*x* + 1, −*y*, −*z*			

4.2. Crystal structures

4.2.1. Crystal structure of $\{[Zn_2(bime)_2(adip)_2]\cdot(H_2O)_5\}_n$ (**1**)

Single-crystal X-ray diffraction analysis reveals that complex **1** crystallizes in the monoclinic space group Pc and is a 2D wavy

4^4-**sql** net of rectangular grids with lattice water molecules. The asymmetric unit of **1** was comprised of two Zn(II) ions, two bime ligands, two adip anions and five lattice water molecules. As shown in Fig. 1a, Zn1 is four-coordinated by two O atoms from two adip anions and two N atoms from two different bime ligands to furnish a distorted tetrahedron geometry (Zn1–O3^{i} = 1.965(3), Zn1–O5 = 1.983(3), Zn1–N1 = 1.983(4), Zn1–N3^{ii} = 2.024(4) Å). The maximum and minimum bond angles for Zn1 are 125.33(17) and 112.26(18)°, respectively. The distortion of the tetrahedron can be indicated by the calculated value of the τ_4 parameter introduced by Yang et al. [30] to describe the geometry of a four-coordinate metal system, which is 0.87 (for ideal tetrahedron $\tau_4 = 1$). The Zn2 is also located in a tetrahedral geometry and coordinated by two N atoms from two bime ligands and two O atoms from two adip ligands (Zn2–O7 = 1.968(3), Zn2–N8 = 1.983(4), Zn2–O2 = 2.019(3), Zn2–N6^{iii} = 2.041(4) Å), which the value of τ_4 is 0.83. Both Zn–N and Zn–O bond lengths are well-matched to those observed in similar complexes [31–33]. According to the stereochemistry terminology [34], the conformation of the bime in **1** belongs to *gauche* with a torsion angle of 47.3(5)° defined by N2–C17–C16–N4 atoms. The flexible adip shows a *anti-anti-anti* conformation due to three torsion angles of the carbon chain of being 178.6(4), 178.3(5) and 175.8(4)°.

The Zn(II) ions are bridged by μ_2-bime and μ_2-η^1,η^1-adip ligands to form a 2D infinite undulated sheet (Fig. 1b) incorporating a $[Zn_4(bime)_2(adip)_2]$ window of 8.21 × 11.39 Å (Fig. 1c) based on the Zn···Zn distances. This sheet exhibits an undulated character with a thickness of about 7.04 Å (Fig. S1). To better understand the structure of **1**, the topological analysis approach is employed. If all nodes in one net have the identical connectivity, then according to Wells it is a *platonic uniform net* and can be represented by the symbol (n, p), where n is the size of the shortest circuit and p is the connectivity of the nodes [35]. In the sheet of **1**, all Zn(II) ions are 4-connecting and the shortest circuit is a four-membered ring. So this 2D sheet can be simplified to a 4^4-**sql** net.

The most fascinating feature of **1** is that five crystallographically independent lattice water molecules (O1W, O2W, O3W, O4W and O5W) within the void are hydrogen bonded to each other, forming an infinite water chain with a curl conformation (Fig. 1d). The arrangement mode of five water molecules within a water chain can be described as ···O1W···O4W···O2W···O5W···O3W···O1W···O4W···O2W···O5W···O3W···. The O···O distances in the chain are in the range 2.789(7)–2.907(7) Å with an average value of 2.838(7) Å. Moreover, the average O···O···O angle is 133.56(2)°, which is slightly larger than the corresponding value of 109.3 in ice I_h. The water aggregates in **1** can be seen as intercalation of guests into voids of the 3D framework host. (Symmetry codes: (i) $x, y + 1, z$; (ii) $x + 1, y, z$; (iii) $x - 1, y, z$.)

4.2.2. *Crystal structure of* $\{[Zn(bime)(ipa)]\cdot(H_2O)_3\}_n$ *(**2**)*

When using H_2ipa instead of the H_2adip, we obtained a similar 2D infinite 4^4-**sql** net. Single crystal X-ray analysis reveals that **2** crystallizes in a monoclinic space group $P2_1/c$. As shown in Fig. 2a, there are one Zn(II) ion, one bime ligand, one ipa anion and three lattice water molecules in the asymmetric unit of **2**. The Zn(II) ion adopts a distorted tetrahedron geometry completed by two N atoms from two bime ligands and two O atoms from two ipa anions with the value of τ_4 being 0.89. The bond lengths and

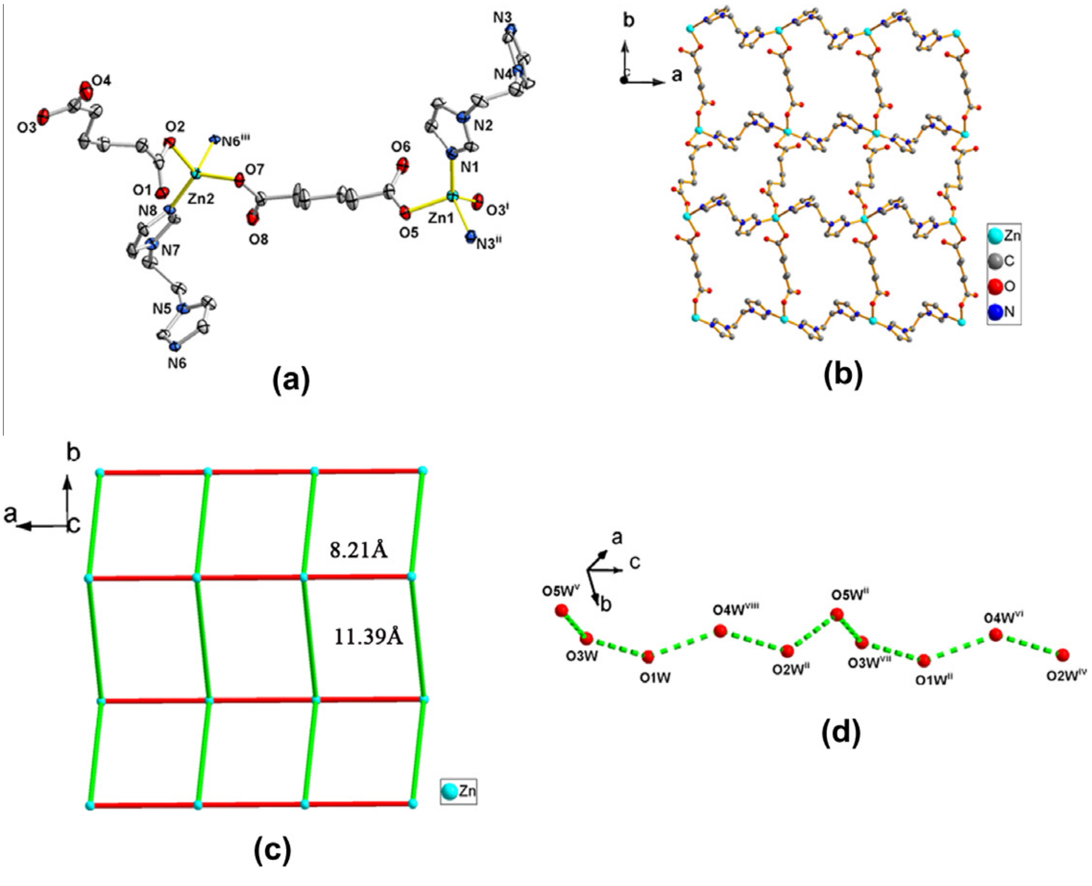

Fig. 1. (a) The coordination environment of the Zn(II) ion and the linkage modes of ligands in **1** with 50% thermal ellipsoid probability. Hydrogen atoms are omitted for clarity. (b) The 2D sheet structure along c axis. (c) Representation of the 4^4-**sql** net (red stick: adip; green stick: bime). (d) The structure of 1D water chain in **1**. (For interpretation of the references to color in this figure legend, the reader is referred to the web version of this article.)

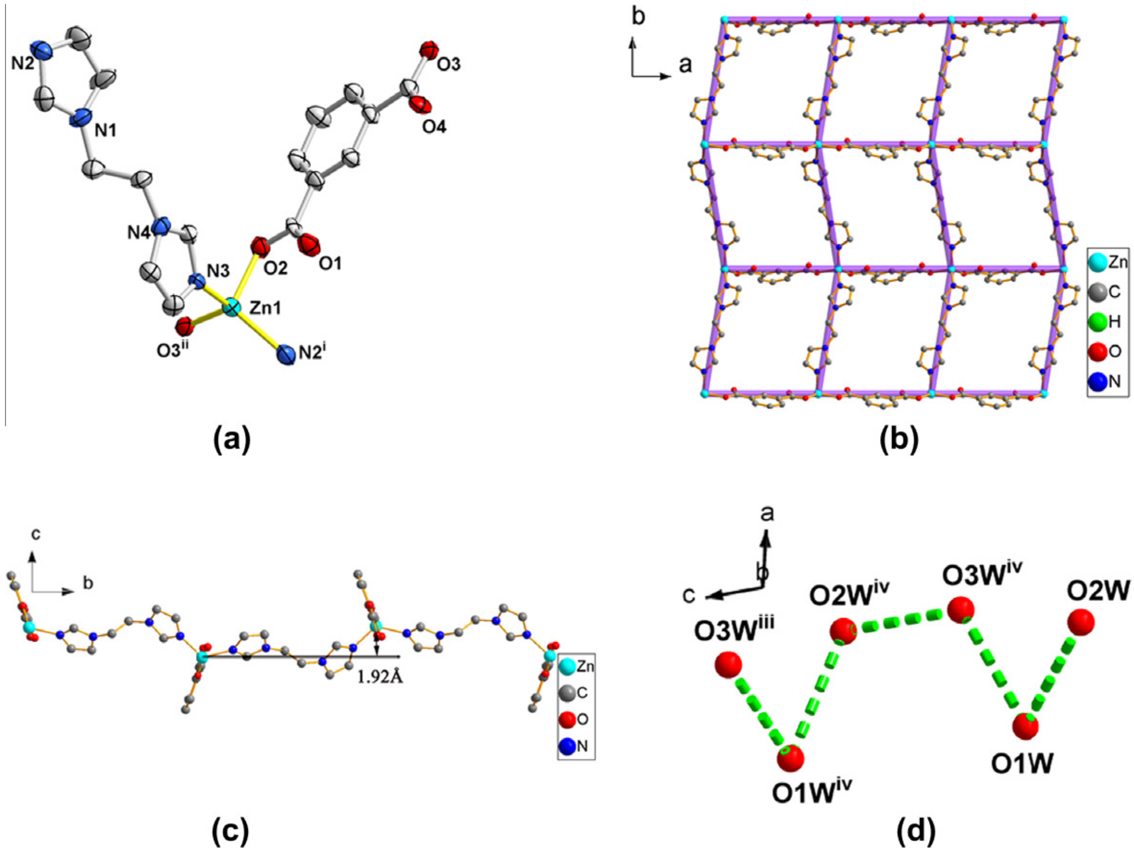

Fig. 2. (a) The coordination environment of the Zn(II) ion and the linkage modes of ligands in **2** with 50% thermal ellipsoid probability. Hydrogen atoms are omitted for clarity. (b) A view of the 2D 4^4-**sql** net in the structure of **2**. (c) Side view of the single 4^4-**sql** net in the structure of **2**. (d) The structure of 1D water chain in **2**.

bond angles around Zn(II) ion fall in the range of 1.992(7)–2.021(6) Å and 100.7(2)–123.4(3)°, respectively. The conformation of the bime in **2** is *anti* which is different from that of in **1** with a torsion angle of 166.1(7)°. Similar to **1**, the basic structure of **2** is also a 4^4-**sql** net which is constructed by Zn(II) ions, bidentate bime and ipa ligands (Fig. 2b). This 4^4-**sql** net also contains one type of node (four-connected Zn(II) ions) and two types of linkers (two-connected bime and ipa ligands). Compared to the net of **1**, the net in **2** contains a larger window of 10.23 × 11.33 Å which is due to the different conformations of bime. The bime belonging to an *anti* conformation in **2** is much longer than that in **1** with *gauche* conformation. Meanwhile, the net exhibits a slightly undulated character with a thickness of about 1.92 Å (Fig. 2c).

There is also a 1D infinite water chain in **2** and a clear insight into this water structure is shown in Fig. 2d. Three crystallographically independent lattice water molecules (O1W, O2W and O3W) and their symmetry-related ones compose of the 1D water chain by H-bonds. O1W and O2W act as hydrogen donors to bond with carboxylate oxygen atoms O1 and O4 from coordination sheet, respectively. As a result, the water chains serve as "glue" to reinforce the 2D sheets forming an overall 3D supramolecular framework. The O···O distances in the chain are in the range 2.65(2)–2.847(15) Å with an average value of 2.752(6) Å, moreover, the O···O···O angles fall in the range 84.93(5)–119.01(5)°.

4.2.3. Crystal structure of $\{[Zn(bime)(tpa)]\cdot(H_2O)\cdot(CH_3OH)\}_n$ (**3**)

Complex **3** crystallizes in the triclinic space group *P*-1. As shown in Fig. 3a, the asymmetric unit of **3** contains one independent Zn(II) ion, one bime ligand, one tpa anion, one lattice water molecule and one uncoordinated methanol molecule. The Zn(II) ion is bound by two N atoms from two bime ligands and two O atoms from two tpa anions to complete a tetrahedron geometry (Zn1–O3 = 1.9494(15), Zn1–O2 = 1.9901(15), Zn1–N1 = 2.0101(19), Zn1–N4^i = 1.9957(19) Å). The maximum and minimum bond angles for Zn(II) ion are 115.31(7) and 97.21(7)°, respectively. The conformation of the bime in **3** is the same to that of in **1** with a torsion angle of 54.6(2)°. As shown in Fig. 3b, the bime acts as a bidentate ligand and the tpa adopts a μ_2-η^1,η^1 coordinated mode which links the Zn(II) ions to form a 2D sheet. To better understand the structure of **3**, the topological analysis is employed [36]. We can consider the Zn(II) ions as 3-connecting nodes, and each two neighboring Zn(II) ions were linked via bridging ligands (bime or tpa ligand) to form Zn_6 hexagonal rings. On the basis of above analysis, the 2D structure can be simplified to a hexagonal 6^3-**hcb** net with the grid dimensions of 7.32 × 10.97 Å (Fig. 3c). The uncoordinated methanol molecules and lattice water molecules are filled in the windows and hydrogen-bonded to carboxyl groups to extend the 2D sheet to 3D supramolecular framework. (Symmetry codes: (i) $-x + 1, -y, -z$.).

4.3. Effect of bime and dicarboxylates ligands on assembly

As it is shown in the descriptions above, three novel Zn(II) CPs **1**–**3** with the bime and different dicarboxylates were successfully synthesized and characterized. Based on the X-ray analysis results, although **1** and **2** have the similar 2D infinite 4^4-**sql** net structure, they contain different sizes of windows. For **1** and **2**, the auxiliary dicarboxylates (adip and ipa) with the same μ_2-η^1,η^1 coordination mode possess different lengths and the main ligand bime adopts the identical μ_2 bridging coordination mode but belonging to different conformations with different lengths. The structure of **3** is a 2D sheet which can be simplified to a hexagonal 6^3-**hcb** net with the grid dimensions of 7.32 × 10.97 Å. In **3**, the bime acts as a

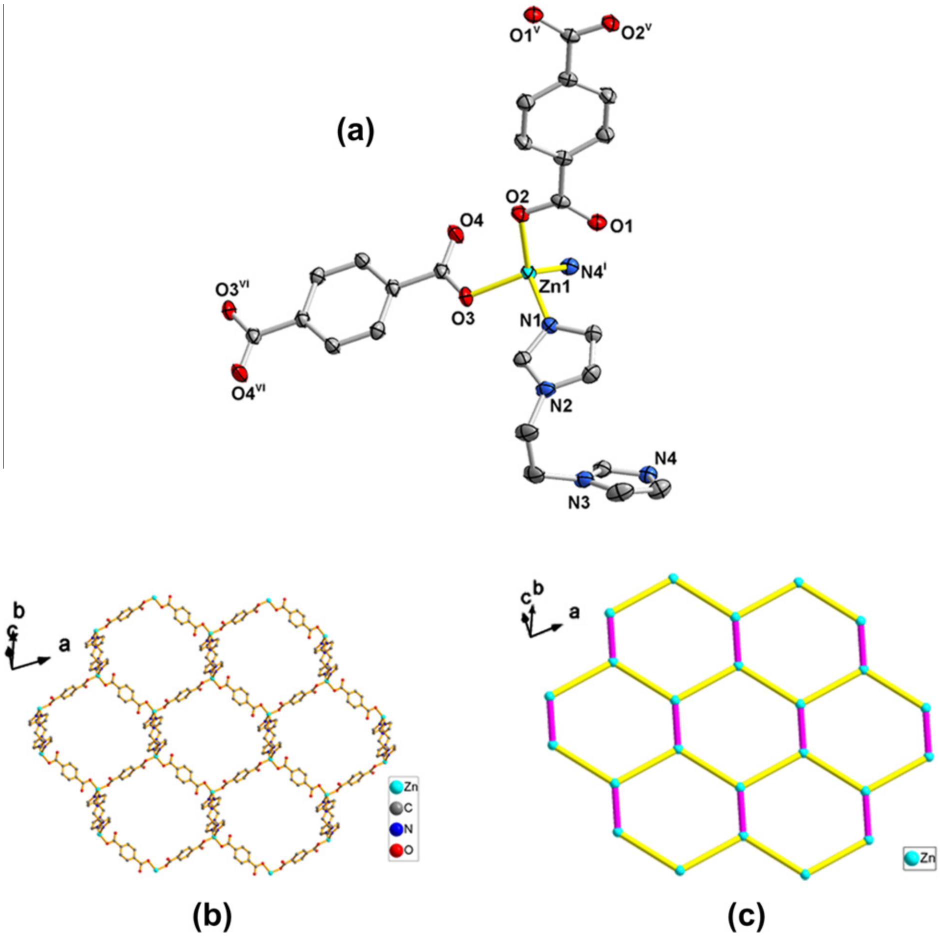

Fig. 3. (a) The coordination environment of the Zn(II) ion and the linkage modes of ligands in **3** with 50% thermal ellipsoid probability. Hydrogen atoms are omitted for clarity. (b) The 2D sheet structure. (c) Representation of the hexagonal 6^3-**hcb** net grid (yellow stick: tpa; amaranth stick: bime). (For interpretation of the references to color in this figure legend, the reader is referred to the web version of this article.)

bidentate ligand with a *gauche* conformation and the tpa adopts a μ_2-η^1,η^1 coordinated mode. In all, the different auxiliary dicarboxylates as well as bime with different conformations significantly contributed to the different structures of **1**–**3**.

4.4. Photoluminescence properties

The photoluminescence spectra of the complexes **1**–**3** are shown in Fig. 4. The free ligand bime displays photoluminescence with emission maximum at 356 nm (λ_{ex} = 300 nm, Fig. S2). It can be presumed that this peak originate from the $\pi^* \rightarrow \pi$ transition. To the best of our knowledge, the emission of dicarboxylate belongs to $\pi^* \rightarrow n$ transitions which is very weak compared to that of the $\pi^* \rightarrow \pi$ transition of the bime, so the dicarboxylates almost have no contribution to the fluorescent emission [37]. Upon complexation of these ligands with Zn(II) ions, intense emissions are observed at 427 nm for **1**, 433 nm for **2** and 436 nm for **3**, under 300 nm excitation, respectively. The resemblance between the emissions of **1**–**3** and that of the free bime indicates that the emissions of **1**–**3** originate from $\pi^* \rightarrow \pi$ electronic transition of bime ligand.

4.5. X-ray powder diffraction analyses and thermal analyses

Powder X-ray diffraction (PXRD) has been used to check the phase purity of the bulky samples in the solid state. For **1**–**3**, the measured PXRD patterns closely match the simulated patterns generated from the results of single-crystal diffraction data (Fig. S3), indicative of pure products. The Thermogravimetric (TG) analysis was performed in N_2 atmosphere on polycrystalline samples of **1**–**3**. As shown in Fig. 5, in **1**, the framework is stable to 350 °C and then the framework begins to collapse, accompanying the release of coordinated bime and ipa ligands. There exists a gradual weight loss of **2** occurring from 30 to 200 °C which is

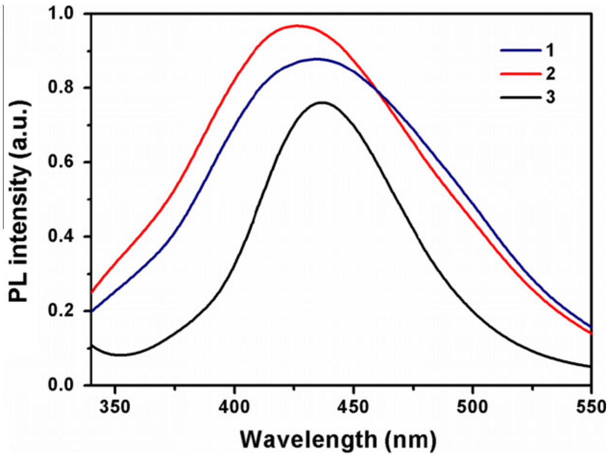

Fig. 4. Emission spectra of the complexes **1**–**3**.

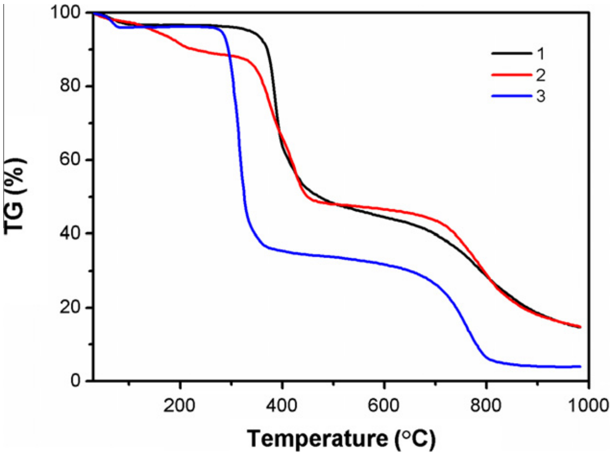

Fig. 5. TGA curves for complexes **1**–**3**.

attributed to the loss of uncoordinated water molecules. The weight loss is about 11.3%, in correspondence with the calculated value of 12.0%. Its framework is stable to 330 °C and then the framework begins to collapse, accompanying the release of coordinated bime and ipa ligands. For **3**, a weight loss occurred from 30 to 100 °C which is attributed to the loss of uncoordinated water molecule. The weight loss is about 3.9%, in correspondence with the calculated value of 4.0%. The framework keeps stable to 360 °C, and then the framework collapses accompanying the release of the bime and carboxylate ligands.

5. Conclusions

In conclusion, we prepared and characterized three novel mixed-ligand Zn(II) complexes which constructed from the bime and dicarboxylic acid. Complexes **1** and **2** have the similar 2D infinite (4,4) net structures in which two different hydrogen-bonded water chains were also observed and **3** is a 2D hexagonal 6^3-**hcb** net structure. For **1–2**, bime adopts the identical μ_2 bridging coordination mode but belonging to different conformations with different lengths. In **2**, the bime belongs to a *anti* conformation which is much longer than that in **1** with *gauche* conformation. As a result, complex **2** possesses a larger (4,4) net than that in **1**. Compared **1** with **3**, although the bime adopts the same conformations, they obtain 2D (4,4) net and 6^3-**hcb** net, respectively, which is due to the influence of different dicarboxylates. The results of this study not only demonstrate that the conformation of the bime ligands may tune the frameworks of coordination complex but also illustrate that the various dicarboxylates may also play an important role in the formation of final structures.

Acknowledgments

This work was financially supported by the National Natural Science Foundation of China (No. 20721001), 973 Project (Grant 2007CB815301) from MSTC, Independent Innovation Foundation of Shandong University (2011GN030), and the Special Fund for Postdoctoral Innovation Program of Shandong Province (201101007).

Appendix A. Supplementary material

CCDC 853480, 853481 and 853482 contain the supplementary crystallographic data for **1–3** respectively in this paper. These data can be obtained free of charge via http://www.ccdc.cam.ac.uk/conts/retrieving.html, or from the Cambridge Crystallographic Data Centre, 12 Union Road, Cambridge CB 21EZ, UK; fax: (+44) 1223-336-033; or e-mail: deposit@ccdc.cam.ac.uk. Supplementary data associated with this article can be found, in the online version, at doi:10.1016/j.molstruc.2011.12.030.

References

[1] G. Férey, Chem. Soc. Rev. 37 (2008) 191.
[2] S.L. James, Chem. Soc. Rev. 32 (2003) 276.
[3] E.B. Rusanov, V.V. Ponomarova, V.V. Komarchuk, H. Stoeckli-Evans, E. Fernandez-Ibanez, F. Stoeckli, J. Sieler, K.V. Domasevitch, Angew. Chem., Int. Ed. 42 (2003) 2499.
[4] A.J. Lan, K.H. Li, H.H. Wu, D.H. Olson, T.J. Emge, W. Ki, M.C. Hong, J. Li, Angew. Chem., Int. Ed. 48 (2009) 2334.
[5] J.P. Zhang, X.C. Huang, X.M. Chen, Chem. Soc. Rev. 38 (2009) 2385.
[6] M.J. Zaworotko, Nature 451 (2008) 410.
[7] T.L. Hennigar, P. Losier, D.C. MacQuarrie, M.J. Zaworotko, R.D. Rogers, Angew. Chem., Int. Ed. Engl. 36 (1997) 972.
[8] G.J. McManus, J.J.P. Iv, M. Perry, B.D. Wagner, M.J. Zaworotko, J. Am. Chem. Soc. 129 (2007) 9094.
[9] L. Tei, V. Lippolis, A.J. Blake, P.A. Cooke, Chem. Commun. (1998) 2633.
[10] E.C. Constable, T. Kulke, G. Baum, D. Fenske, Chem. Commun. (1997) 2043.
[11] D.J. Eisler, R.J. Puddephatt, Inorg. Chem. 45 (2006) 7295.
[12] D. Venkataraman, Y. Du, S.R. Wilson, K.A. Hirsch, P. Zhang, J.S. Moore, J. Chem. Educ. 74 (1997) 915.
[13] G. Baum, E.C. Constable, D. Fenske, C.E. Housecroft, T. Kulke, M. Neuburger, M. Zehnder, J. Chem. Soc., Dalton Trans. (2000) 945.
[14] Y. Chen, H.X. Li, D. Liu, L.L. Liu, N.Y. Li, H.Y. Ye, Y. Zhang, J.P. Lang, Cryst. Growth Des. 8 (2008) 3810.
[15] M.T. Rispens, A. Meetsma, R. Rittberger, C.J. Brabec, N.S. Sariciftci, J.C. Hummelen, Chem. Commun. (2003) 2116.
[16] W.H. Zhang, Y.L. Song, Y. Zhang, J.P. Lang, Cryst. Growth Des. 8 (2008) 253.
[17] G. Smith, B.A. Cloutt, D.E. Lynch, K.A. Byriel, C.H.L. Kennard, Inorg. Chem. 37 (1998) 3236.
[18] Y. Kang, S.S. Lee, K.M. Park, S.H. Lee, S.O. Kang, J. Ko, Inorg. Chem. 40 (2001) 7027.
[19] J. Seo, M.R. Song, K.F. Sultana, H.J. Kim, J. Kim, S.S. Lee, J. Mol. Struct. 827 (2007) 201.
[20] O.S. Jung, Y.J. Kim, Y.A. Lee, K.M. Park, S.S. Lee, Inorg. Chem. 42 (2003) 844.
[21] X.L. Wang, C. Qin, E.B. Wang, Y.G. Li, Z.M. Su, L. Xu, L. Carlucci, Angew. Chem., Int. Ed. 44 (2005) 5824.
[22] P.Q. Zheng, Y.P. Ren, L.S. Long, R.B. Huang, L.S. Zheng, Inorg. Chem. 44 (2005) 1190.
[23] D. Sun, Z.H. Wei, C.F. Yang, D.F. Wang, N. Zhang, R.B. Huang, L.S. Zheng, Cryst. Eng. Commun. 13 (2011) 1591.
[24] X.C. Huang, J.P. Zhang, Y.Y. Lin, X.L. Yu, X.M. Chen, Chem. Commun. (2004) 1100.
[25] F.H. Allen, Acta Crystallogr., Sect. B: Struct. Sci. 58 (2002) 380.
[26] Cambridge Structure Database Search, CSD Version 5.28 (November 2006) with 15 Updates (January 2007–November 2011).
[27] G.M. Sheldrick, SHELXS 97: Program for Crystal Structure Solution, University of Göttingen, Germany, 1997.
[28] G.M. Sheldrick, SHELXL 97: Program for Crystal Structure Refinement, University of Göttingen, Germany, 1997.
[29] K. Nakamoto, Infrared and Raman Spectra of Inorganic and Coordination Compounds, John Wiley & Sons, New York, 1986.
[30] L. Yang, D.R. Powell, R.P. Houser, Dalton Trans. (2007) 955.
[31] X. Zhao, H. He, T. Hu, F. Dai, D. Sun, Inorg. Chem. 48 (2009) 8057.
[32] H. He, F. Dai, D. Sun, Dalton Trans. (2009) 763.
[33] X. Zhao, H. He, F. Dai, D. Sun, Y. Ke, Inorg. Chem. 49 (2010) 8650.
[34] G.P. Moss, Pure Appl. Chem. 68 (1996) 2193.
[35] A.F. Wells, Three-Dimensional Nets and Polyhedra, Wiley-Interscience, New York, 1977.
[36] B.F. Hoskins, R. Robson, J. Am. Chem. Soc. 112 (1990) 1546.
[37] W.J. Chen, Y. Wang, C. Chen, Q. Yue, H.M. Yuan, J.S. Chen, S.N. Wang, Inorg. Chem. 42 (2003) 944.